# DEM-SIMULATION OF MAGNETIC FIELD EFFECTS IN SOLID-LIQUID-SEPARATION

Dipl.-Ing. Christian Eichholz, Prof. Dr.-Ing. Hermann Nirschl

Institute for Mechanical Engineering and Mechanics, University of Karlsruhe (Karlsruhe Institute of Technology), Germany, christian.eichholz@mvm.uni-karlsruhe.de

**Abstract**

This paper presents a numerical study of the cake formation and growth in the magnetic field enhanced cake filtration by means of the Discrete Element Method (DEM). The process of magnetic field enhanced cake filtration results from the combination of classical cake filtration and magnetic field driven separation. Experimental results prove that different magnetic field effects influence the filtration process positively. In the present paper the DEM-Simulation gives further insight in the mechanisms of structuring effects of the filter cake and especially the interaction of magnetic, hydrodynamic and mass forces. The motion of the discrete particles is obtained by applying the three-dimensional Newton's laws of motion to every single particle. Beside external forces particle interactions are calculated using the modified DLVO-theory. Liquid phase flow is assumed as one-dimensional. Although the simulation results only represent a small cut-out the numerical results can be assigned to the same regimes of liquid flow and magnetic field effects that are observed experimentally.

**Keywords**

Solid-Liquid-Separation, Cake Filtration, Magnetic Filtration, Magnetic Structuring, Simulation, Discrete Element Method

## 1. INTRODUCTION

The basic idea of the Discrete Element Method (DEM) is to solve the Newton's laws of motion for all N discrete elements of the system for all degrees of freedom to describe the motion of all particles individually. Occurring forces are categorized into primary and secondary forces. Primary forces are external and interaction forces between pairs of particles. Secondary forces are contact forces which describe the effect of particle collisions (Johnson 1985; Deen et al. 2007). The time depending integration of Newton's laws has to be accomplished numerically. Independently from the integration method the time step has to be chosen in a manner that in each iteration step constant forces can be assumed. Two different approaches for describing the particle contact can be found in literature. The hard-sphere approach as a quite fast method can be used for diluted systems. Only binary collisions can be regarded one after the other although they might occur simultaneously. The conditions after an impact are calculated according to the Hertz contact theory. For multi body contacts the soft-sphere approach has turned out to be more helpful. Collisions are not calculated immediately but tracked over the whole time step. This way several contacts of one particle can be treated. The collision is described by a virtual overlapping of the spheres. Only after detecting all particle contacts in one time step the Newton equations are integrated.

The process of magnetic field enhanced cake filtration results from the combination of classical cake filtration and magnetic field driven separation. Experimental results prove that different magnetic field effects influence the filtration process positively (Fuchs et al. 2006; Eichholz et al. 2008). In inhomogeneous magnetic fields magnetic particles experience a magnetic force. That gives the possibility to decouple solid and liquid phase motion. In case of counter wise orientation of differential pressure and magnetic force this leads to a decrease of the rate of cake formation, implying a smaller packed bed that the liquid phase has to drain and thus a reduction in filtration resistance. If the field strength is high enough even the prevention of cake formation at the beginning of a filtration process is possible. Thereby the filter media is kept free of particles and the filtrate can run through the filter media almost without resistance. Only after the outflow of the excess water the particles deposit on the filter media.
The magnetic force not only has an impact on the cake built-up but also on the structure of the filter cake. Exposed to a homogeneous or inhomogeneous magnetic field magnetic particles form North and South Poles and act as microscopic magnets themselves. Resulting interparticle forces upon approaching particles lead to formation of chainlike agglomerates in direction of the external magnetic field while particles orientated perpendicular to the field direction experience a repulsive force (Chin et al. 2000). Obviously the permeability of a cake with this channeled structure is higher than the one of a filter cake from classical filtration. Together these effects result in a strong improvement of filtration kinetics and thus in a reduction of the filtration resistance.

## 2. PHYSICAL BACKGROUND

### *2.1 Forces on Particles*

Primary forces acting on the particles can be divided into external forces acting on each particle depending on its absolute position in the apparatus or simulation area, respectively, and into interaction forces between neighbouring particles. In the present case external forces that are regarded are gravity, buoyancy, hydrodynamic, and external magnetic forces (eq.2-4). The filtrate velocity decreases with time because of the increasing filter cake resistance of the deposited particles. The velocity is calculated with Ruth's law and the approach of Karman-Cozeny for the permeability $P_c$ of filter cakes. Usually the Karman-Cozeny constant is assumed as 180. A more detailed approach breaks this value down to a constant for the pore geometry and the tortuosity $\tau$. The latter is a quantity to describe the straightforwardness of the pore structure in a filter cake (eq.1). Typically its value is $\tau = \sqrt{2}$ (Sorrentino 2002).

$$\tau = \frac{L_{eff}}{h_c} \qquad (1)$$

Usually in a liquid phase forces between particles are described by the DLVO-theory. For magnetized particle systems a modified DLVO-theory is suggested that also accounts for magnetic particle interactions (Chin et al. 2000). Considered forces are in detail electrostatic repulsion, van der Waals attraction, Born repulsion and magnetic dipole forces (eq. 5-7). The constant $H_0$ in the van de Waals force is referred to as Hamaker constant. Available data from literature defines an interval for the constant of $0.3\text{-}1.4 \cdot 10^{-20}$ J for polymer materials (Lagaly et al. 1997). In this work the magnitude of $H_0$ is assumed in the same region. Short range or Born repulsion is represented by defining a minimum distance between the two surfaces in the calculation of the attractive van der Waals interactions (Kim, Hoek 2002). Magnetic particles in a magnetic field attract and align in field direction but experience a

repulsive force perpendicular to this direction. Satoh (Satoh et al. 1998) introduces a vectorial notation, which comprises both, attractive and repulsive effects (eq. 7).

$$\vec{F}_{g,b} = V \cdot \Delta\rho_{sl} \cdot \vec{g} \tag{2}$$

$$\vec{F}_{hyd} = 3 \cdot \pi \cdot \eta \cdot d \cdot (\vec{v}_{\infty} - \vec{v}) \tag{3}$$

$$\vec{F}_{m,ext} = V \cdot \rho \cdot M \cdot \nabla \vec{B} \tag{4}$$

$$\vec{F}_{elec,ij} = \frac{128 \cdot \pi \cdot N_A \cdot c_{ion,\infty} \cdot k \cdot T}{\kappa^2} \cdot \frac{d_i \cdot d_j}{4} \cdot \gamma_i \cdot \gamma_j \cdot \left( \frac{1}{r_{ij}^2} - \frac{\kappa}{r_{ij}} \right) \cdot \exp\left\{ -\kappa \cdot \left( r_{ij} - \frac{d_i + d_j}{2} \right) \right\} \cdot \vec{n}_{ij} \tag{5}$$

$$\vec{F}_{vdW,ij} = -\frac{H_0}{6} \cdot r_{ij} \cdot d_i \cdot d_j \cdot \left[ \frac{1}{r_{ij}^2 - \left( \frac{d_i + d_j}{2} \right)^2} - \frac{1}{r_{ij}^2 - \left( \frac{d_i - d_j}{2} \right)^2} \right]^2 \cdot \vec{n}_{ij} \tag{6}$$

$$\vec{F}_{m,dip,ij} = -\frac{3 \cdot \pi \cdot \mu_0 \cdot \rho_s^2 \cdot d_i^3 \cdot d_j^3}{144} \cdot \frac{M_i \cdot M_j}{r_{ij}^4} \cdot \left[ -\langle \vec{m}_i \cdot \vec{m}_j \rangle \cdot \vec{n}_{ij} + 5 \cdot \langle \vec{m}_i \cdot \vec{n}_{ij} \rangle \cdot \langle \vec{m}_j \cdot \vec{n}_{ij} \rangle \cdot \vec{n}_{ij} - \langle \vec{m}_j \cdot \vec{n}_{ij} \rangle \cdot \vec{m}_i - \langle \vec{m}_i \cdot \vec{n}_{ij} \rangle \cdot \vec{m}_j \right] \tag{7}$$

### *2.2 Structuring Effects*

To quantify the structure of a filter cake formed in the magnetic field an energy ratio $E_S$ can be calculated (Eichholz et al. 2008) similar to the energy ratio for magnetically stabilized fluidized beds suggested by Rosensweig (Rosensweig et al., 1981) (eq.8),

$$E_S = \frac{E_{hyd}}{E_{m,dip}} = \frac{3 \cdot \pi \cdot \eta \cdot d^2 \cdot v}{\frac{1}{144} \cdot \pi \cdot \mu_0 \cdot \rho_s^2 \cdot M^2 \cdot d^3} = \frac{432 \cdot \eta \cdot v}{\mu_0 \cdot \rho_s^2 \cdot M^2 \cdot d} \tag{8}$$

The drag potential $E_{hyd}$ defines the energy that is needed to lift one particle against the drag force $F_{hyd}$ by one particle diameter. This potential describes the hindrance of the magnetically induced particle configuration due to the flow of the liquid phase. The magnetic dipole energy $E_{m,dip}$ is the repulsive energy between two particles in contact perpendicular to the external field direction. For $E_S<1$ the structure is strongly ordered, for $1<E_S<10$ a partly structured and for $E_S>10$ an unstructured bed can be assumed. This parameter can serve as a tool to compare the regimes of experimental and calculated results.

## 3. THE DISCRETE ELEMENT METHOD

### *3.1 Contact Forces*

In the presented work the soft-sphere approach is utilized. A deformation of the spheres in a collision is replaced by an virtual overlap $\lambda$ of the particles which evokes a set of reset forces in normal and tangential direction (Fig.1).

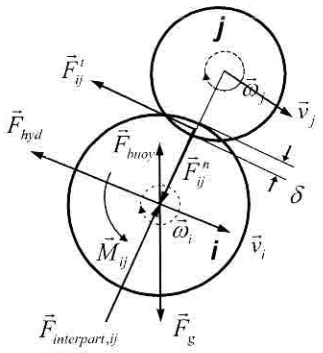


**Fig.1: Particle contact: soft-sphere approach**

The normal contact force results from a parallel connection of a spring and a damping element describing the storage and dissipation of kinetic energy (eq.9) (Fig.2) (Deen et al. 2007; Chu, Yu 2008).

$$\vec{F}_{n,ij} = k_n \cdot \lambda^{1,5} \cdot \vec{n}_{ij} - \eta_{n,ij} \cdot \vec{v}_{rel,n,ij} \qquad (9)$$

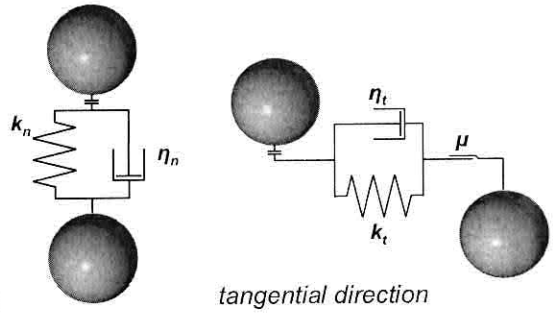


**Fig.2: Particle contact model**

The spring force is a function of the spring stiffness $k_n$. Usually it is calculated applying the Hertz contact theory for spheres. The deformation of the spheres or the overlap, respectively, is described using Young's modulus and Poisson's ratio. Often this value does not reflect the behavior adequately. Thus it is defined, e.g. by fitting it to the occurring force load (Deen et al. 2007; Simsek et al. 2008). In the present work the stiffness is determined by means of a force equilibrium between the maximum force and the spring force allowing a defined overlap $\lambda_0$ (eq.10). The damping coefficient is calculated from the particle mass, the depth of overlap and the spring stiffness (eq.11).

$$k_n = \frac{\left|\vec{F}_{\max}\right|}{\lambda_0^{1.5}} \qquad (10)$$

$$\eta_{n,ij} = c_n \cdot \sqrt{\frac{9}{2} \cdot \left( \frac{m_i \cdot m_j}{m_i + m_j} \right) \cdot \sqrt{\lambda} \cdot k_n} \qquad (11)$$

In tangential direction the modus is similar (eq.12) only a slider element has to be added in serial connection (Fig.2). In each calculation cycle it is checked if Coulomb friction can be applied and particles stick together or if they start sliding (eg.14).

$$k_{t,stat/dyn} = \frac{\mu_{stat/dyn}}{\lambda_0} \cdot \left|\vec{F}_{\max}\right| \tag{12}$$

$$\eta_{t,ij} = 2 \cdot \sqrt{\frac{2}{7} \cdot \left(\frac{m_i \cdot m_j}{m_i + m_j}\right) \cdot k_{t,dyn}} \tag{13}$$

$$\left|\vec{F}_{t,ij}\right| \leq \mu_{stat} \cdot \left|\vec{F}_{n,ij}\right| \tag{14}$$

Relative tangential movement of two particles in contact results in an increase of the spring force (eq.15). If static friction is outranged and particles start moving position and tangential forces have to be updated (eq.16).

$$\vec{F}_{t,ij} = -k_{t,sta} \cdot \Delta x_{t,ij} - \eta_{t,ij} \cdot v_{rel,t,ij} \tag{15}$$

$$\vec{F}_{t,ij} = -\mu_{dyn} \cdot \left|\vec{F}_{n,ij}\right| \vec{t}_{ij} \cdot \Delta x_{t,ij} \tag{16}$$

### *3.2 Boundary Conditions and Integration Method*

The lower border the simulation area is confined by the filter media with a distinguished permeability for the aqueous phase only. The contact between the filter media and a particle also is calculated with the soft-sphere approach. The upper limit is defined by the liquid surface which during filtration. All sides of the simulation area are treated as periodic boundaries. Initial values for filtration pressure, filter media resistance, magnetic field strength and material properties are chosen similar to Eichholz et al. (Eichholz et al. 2008).

According to Beeman (Beeman 1976) the third-order Adams-Bashforth-Moulton algorithm is chosen to integrate the Newton's laws of motion (eq.17, 18). It is a multistep method using a predictor and a corrector step. This way good stability is achieved while avoiding the implicit calculations of the Adams-Moulton approach.

$$m_i = \frac{d\vec{v}_i}{dt} = \vec{F}_i \tag{17}$$

$$I_i = \frac{d\vec{\omega}_i}{dt} = \vec{T}_i \tag{18}$$

Beside the integration method also the time step affects the stability of the calculation. A small time step results in a more stable calculation but also causes larger computation time. In this work convergence is achieved using time steps $\Delta t \leq 1e^{-6}$ s. For calculation efficiency several update frequencies can be chosen for detecting neighboring particles, updating the magnetic moments, analyzing the filtration results (porosity devolution, cake height, filtrate volume) and calculating a new filtration velocity.

## 4. RESULTS

### *4.1 Variation of Filtration Parameters*

In the first stage of developing the program code particle rotation is neglected. The code is tested calculating the influence of filtration pressure on the filtration results without applying a magnetic field. The calculation are only carried out for 300 particles hence the filtration duration is short and the absolute filter cake height only amounts to several particle diameters. But nevertheless the simulation shows a cake built-up as expected from filtration theory (Fig.3).

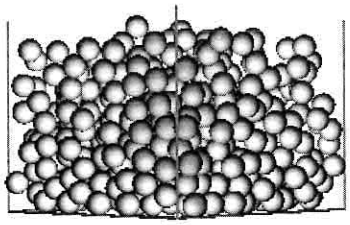

**Fig.3: Picture of filter cake for 1.6bar filtration pressure in 3D-simulation**

The corresponding initial specific filtrate volume can be seen in Fig.4. The solid and the dotted line show the progress of the filtrate volume calculated from filtration theory. Data points are obtained by DEM-simulation with an automatic cake surface detection for the calculation of the filtration resistance.

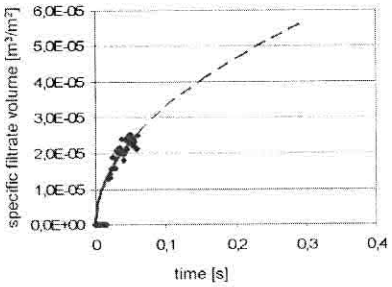


**Fig.4: Initial specific filtrate volume vs. filtration time**

### *4.2 Magnetic Field Influence*

The presented results with a superposed homogeneous magnetic field are calculated without including the DLVO-Theory only regarding a monosized particle distribution. Hence a densest packing of spheres is obtained for classical filtration (Fig.5a). All simulations start with a random particle distribution over the whole simulation area. With increasing magnetic field the filter cake changes to a looser structure (Fig.5b-c).

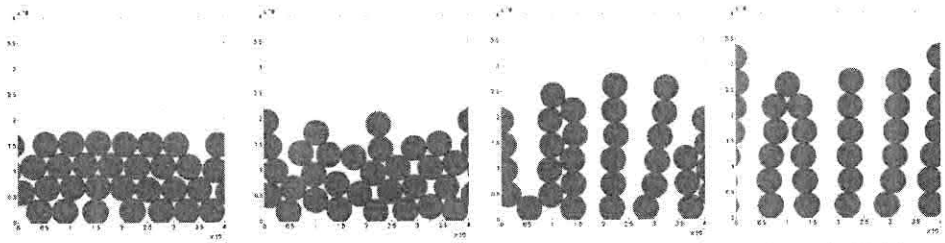

a) $B = 0$ T b) $B = 0.005$ T c) $B = 0.01$ T d) $B = 0.05$ T

**Fig.5: Final particle packing for different magnetic field strengths**

Fig.6 shows the structure parameter $E_s$ (eq.8) calculated from the obtained porosities. For classical filtration the parameter results in a singularity, since the magnetic potential tends to be zero. The principle devolution correlates with experimental results (Eichholz et al. 2008).

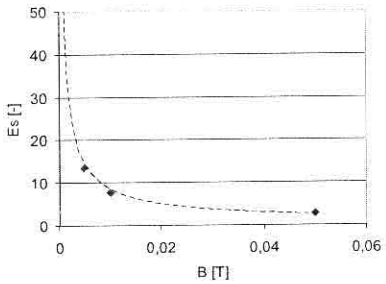


Fig.6: Structure parameter $E_s$ as a function of applied magnetic field

The same effects are observed regarding a larger particle number. In the present case additionally for the determination of the filter cake resistance the tortuosity of the filter cake is calculated as a function of the magnetic field strength (eg.1). Without magnetic field the tortuosity approximates the value already known from literature. With increasing magnetic field strength again the cake gets more structured. Hence the flow channels become more straightforward und the tortuosity decreases.

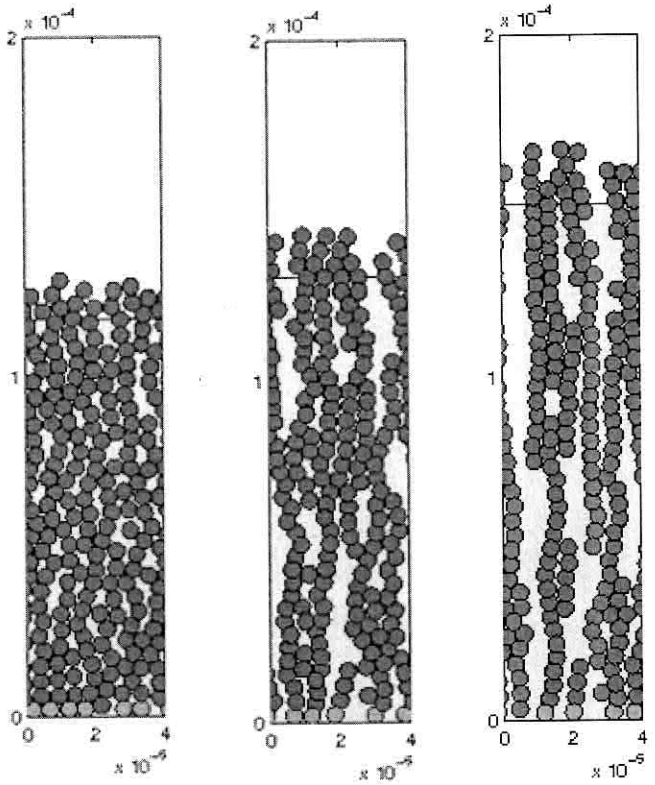


**Fig.7: Final particle packing within the filter cakes and the corresponding tortuosity for different field strengths**

## 5. OUTLOOK

The calculations show the potential of the Discrete Element Method in the simulation of classical and magnetic field enhanced filtration. To achieve more accurate results material properties especially regarding the DLVO-Theory have to be determined more exactly. Furthermore rotational and hydrodynamic effects have to be added to the simulation code.

## 6. ACKNOWLEDGMENT

This work results from cooperation between the University of Karlsruhe and the Massachusetts Institute of Technology. The authors thank the Karlsruhe House of Young Scientists (KHYS) of the Karlsruhe Institute of Technology for their financial support.

## 7. REFERENCES

Beeman, D. (1976); Some Multistep Methods for Use in Molecular-Dynamics Calculations; Journal of Computational Physics 20(2); 130-139

Chin, C. J., Yiacoumi, S., Tsouris, C., Relle, S., Grant, S. B. (2000); Secondary-minimum aggregation of superparamagnetic colloidal particles; Langmuir 16(8); 3641-3650

Chu, K. W., Yu, A. B. (2008); Numerical simulation of complex particle-fluid flows; Powder Technology 179(3); 104-114

Deen, N. G., Annaland, M. V., Van der Hoef, M. A., Kuipers, J. A. M. (2007); Review of discrete particle modeling of fluidized beds; Chemical Engineering Science 62(1-2); 28-44

Eichholz, C., Stolarski, M., Goertz, V., Nirschl, H. (2008); Magnetic field enhanced cake filtration of superparamagnetic PVAc-particles; Chemical Engineering Science 63(12); 3193-3200

Johnson, K. L. (1985); Contact Mechanics; Cambridge, UK; Cambridge University Press

Kim, A. S., Hoek, E. M. V. (2002); Cake structure in dead-end membrane filtration: Monte Carlo simulations; Environmental Engineering Science 19(6); 373-386

Lagaly, G., Schulz, O., Zimehl, R. (1997); Dispersionen und Emulsionen; Darmstadt; Dr. Dietrich Steinkopff Verlag (german)

Satoh, A., Chantrell, R. W., Coverdale, G. N., Kamiyama, S. (1998); Stokesian dynamics simulations of ferromagnetic colloidal dispersions in a simple shear flow; Journal of Colloid and Interface Science 203(2); 233-248

Simsek, E., Wirtz, S., Scherer, V., Kruggel-Emden, H., Grochowski, R., Walzel, P. (2008); An experimental and numerical study of transversal dispersion of granular material on a vibrating conveyor; Particulate Science and Technology 26(2); 177-196

Sorrentino, J. (2002). Advances in correlating filter cake properties with particle collective characteristics. Shaker Verlag. Aachen, Universtität Karlsruhe (TH). Dissertation